Available online at
https://jmeche.uitm.edu.my/

e-ISSN: 2550-164X

Journal of Mechanical Engineering 22(2) 2025, 163 – 172.

Journal of Mechanical Engineering

Simulation-Based Emission Analysis of Electric Turbocompounding in a 1.6L Turbocharged CamPro Engine

MHM Muhammad[1*], AMI Mamat[1], WSAIW Salim[2]

[1]*College of Engineering, School of Mechanical Engineering, Universiti Teknologi MARA, 40450 Shah Alam, Selangor, Malaysia*
[2]*Faculty of Mechanical and Manufacturing, Universiti Tun Hussein Onn Malaysia, 86400 Parit Raja, Batu Pahat, Johor, Malaysia*

ARTICLE INFO

Article history:
Received 21 August 2024
Revised 23 August 2024
Accepted 11 April 2025
Online first
Published 15 May 2025

Keywords:
Electric turbo-compounding
Dual stage turbocharger
Emission
Energy recovery
Internal combustion engine

DOI:
https://doi.org/10.24191/jmeche.v22i2.2928

ABSTRACT

With greenhouse gas emissions (GHG) being the culprit for global warming. Multiple pacts and accords have been made to push countries to increase their efforts towards reducing domestic GHG emissions. The transportation sector accounts for around 20% of global emissions, and new engine architecture needs to be developed for short and midterm solutions. Downsizing and turbocharging engines reduce friction and weight reducing brake-specific fuel consumption through waste heat recovery. The introduction of a low-pressure turbine (LPT) can further recover wasted heat in the exhaust gas by dual-stage turbocompounding. Multiple-stage turbines induce backpressure in the exhaust and can interfere with the combustion process. This can affect the emission of GHG. To investigate this effect, a 1D engine simulation using GT-Power was conducted. A 1.6 L CamPro CFE turbocharged engine was modeled and an electric turcompounding (ETC) unit was added. SI Wiebe combustion model was used to calculate the fraction of fuel burned overtime during the combustion cycle. Two temperature zones were used to further increase emission analysis. The brake-specific gas bsGasi emission was analysed to determine the emitted GHG. The result shows a maximum reduction of 28.8% in $bsGas_{NOx}$, 6.9% in $bsGas_{CO2}$, 7.2% in $bsGas_{CO}$, and 9.9% in $bsGas_{HC}$. Most of the improvements were located at the 3000 – 5000 rpm region with an average of 4% improvement overall. The implementation of ETC successfully reduces the GHG emission while improving the overall efficiency of the engine.

INTRODUCTION

In the 2021 Glasgow Climate Pact, it was agreed that global greenhouse gas (GHG) emissions must be reduced by 45% from 2010 levels by 2030. This has prompted car manufacturers to either enhance the efficiency of their internal combustion engine vehicles or fully transition towards electric vehicles (EVs). Even though a lot of automakers are focusing more on EVs, there hasn't been enough infrastructure built to

[1*] Corresponding author. *E-mail address*: mhanif76@uitm.edu.my
https://doi.org/10.24191/jmeche.v22i2.2928

accommodate EVs, and still considered as early development (Benmouna et al., 2024). Even though the number of EV passenger vehicles has increased in number, this is not the case for heavy vehicles (Crippa et al., 2024). Transport contributes 21.1% of GHG emissions, where nearly one-third are from heavy-duty transport (European Automobile Manufacturers' Association, 2020). Therefore, enhanced spark ignition (SI) engines are still viewed as a practical solution for short- to mid-term improvement.

One novel strategy for lowering SI engine exhaust emissions is to reduce the engine size and install a very effective turbocharging technology. For a specific application, turbocharging provides the advantage of reducing emissions while delivering performance comparable to that of a naturally aspirated (NA) engine (Mahmoudi et al., 2017). Movahed et al. (2014) found that nitrogen oxide (NOx) emissions from a turbocharged engine can be reduced by up to 66% compared to an NA engine. Engine boosting also decreases emissions of carbon dioxide (CO2), carbon monoxide (CO), and unburned hydrocarbons (HC) (Pakale & Patel, 2015; Silva et al., 2009). Carapellucci & Di Battista (2023) model-based evaluation results show an average power recovery of 6% and a reduction of CO_2 emissions of 45 g/kWh by using an additional turbine. However, the most effective boosting method largely depends on the specific application and the complexity of the system (Alshammari et al., 2019). The extremely downsized engine faces a turbo lag issue that limits the turbocharging system's ability to maintain high efficiency at certain engine speeds, despite the benefits of lighter weight, lower engine speed, reduced friction, and enhanced performance.

With the development of low-pressure turbine (LPT), a secondary stage turbine can be placed after the primary turbo to further recover the remaining exhaust gas. Serrano et al. (2022) show that replacing Exhaust Gas Recirculation (EGR) with a secondary turbine extracts more heat recovery and also reduces fuel consumption. Muhammad et al. (2018) preliminary study, utilizing a 1 kW generator attached to an LPT can result in a 2.28% reduction in BSFC and higher thermal efficiency. The addition of a secondary system can be attached to electrical generators as an electrical turbocompounding solution. The recovered energy can be stored and used to power an electric turbocharger, helping to eliminate turbo lag from the primary turbocharger.

However, the two-stage arrangement will have an impact on the combustion process and exhaust emission. This article will look at how electric turbocompounding (ETC) affects the turbocharged CamPro engine's exhaust emissions. This will give a better understanding of the control method to optimize the wastegate (WG) to achieve better brake-specific emission while improving Brake Specific Fuel Consumption (BSFC).

METHODOLOGY

In order to study the emission improvement of dual-stage turbocompounding, a model of an original engine with single turbocharging was used. The engine used the Proton 1.6 L CamPro CFE turbocharged engine. This model was developed based on a validated engine model developed by Ismail et al. in GT-Power (Ismail et al., 2015). However, the engine model developed by Ismail et al. did not focus on emissions analysis. To include complete emission analysis from the engine model, the combustion model needed to be changed to the SI Wiebe Combustion Model. It may be the best model used to forecast the burn rate and burn fraction in internal combustion engines running on various fuels and combustion systems (Ghojel, 2010). Equation 1 shows a general form of the Wiebe function to describe the mass fraction burned with respect to the crank angle:

$$x_b = 1 - exp\left[a\left(\frac{\theta - \theta_0}{\Delta\theta}\right)^{m+1}\right] \tag{1}$$

https://doi.org/10.24191/jmeche.v22i2.2928

where θ is the crank angle, θ_0 is the start of combustion, $\Delta\theta$ is the total combustion duration and a is the extent of complete combustion and m is the burn rate. For the simulation, the fixed parameter uses the same value from the original model.

To increase the accuracy of the predicted emission values, the number of temperature zones was set to two. This will enhance the accuracy of heat release rate measurements and improve the calculations of NOx and HC emissions. (Lakshminarayanan, 2024). Table 1 presents the engine model specifications. The fuel used was RON95, with standard atmospheric air conditions applied for the environment.

The second engine's architecture update includes the addition of the ETC unit downstream of the first turbine outlet. The new engine's layout with the added ETC is seen in Fig 1. The data from Mamat et al. (2016) served as the basis for the ETC turbine's performance maps. Without the use of a wastegate, the ETC is connected directly to an electric generator. The energy recovered was not redirected back into the engine. Fig 2 displays the final layout of the engine model. The engine model was operated at maximum load. To meet the DC electric generator standard, the electric generator was modelled after the "MotorGenerator" available in the GT-Power library, utilizing "voltage-rpm" as the controller. Table 2 provides the electric generator's detailed specifications.

Table 1. Proton 1.6 L CamPro CFE engine specifications

Attribute (Engine)	Value
Combustion system	4-stroke, in-line, gasoline PFI
Capacity	1.6 litres
Compression ratio	9.0
Bore x stroke	76 x 86 mm
Induction system	Single-stage turbocharger
Maximum torque	205 Nm @ 2000-4000 rpm
Maximum power	103 kW @ 5000 rpm
Intake cam profile	≤ 220° (duration) / 7.51 mm (valve lift)
Exhaust cam profile	2° BTDC @ 0.15 mm lift

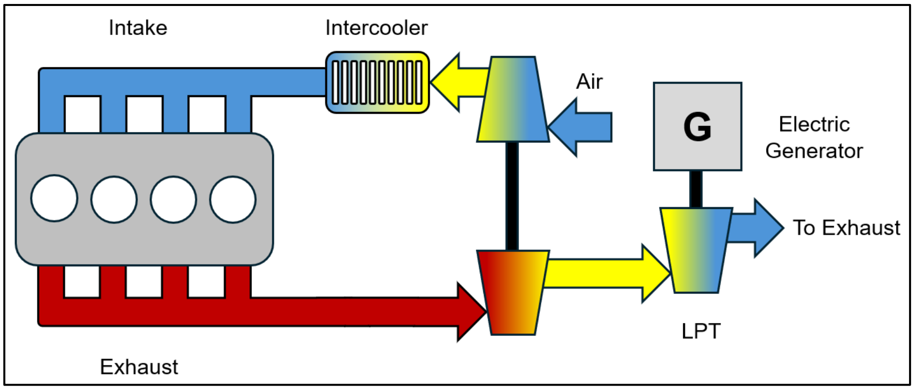

Fig. 1. Dual-stage waste heat recovery using LPT.

Table 2. Electric turbocompounding unit specifications

Specification	Value
Motor voltage	15 V
Shaft speed	50,000 rpm
Current	44 A
Peak current	70 A

https://doi.org/10.24191/jmeche.v22i2.2928

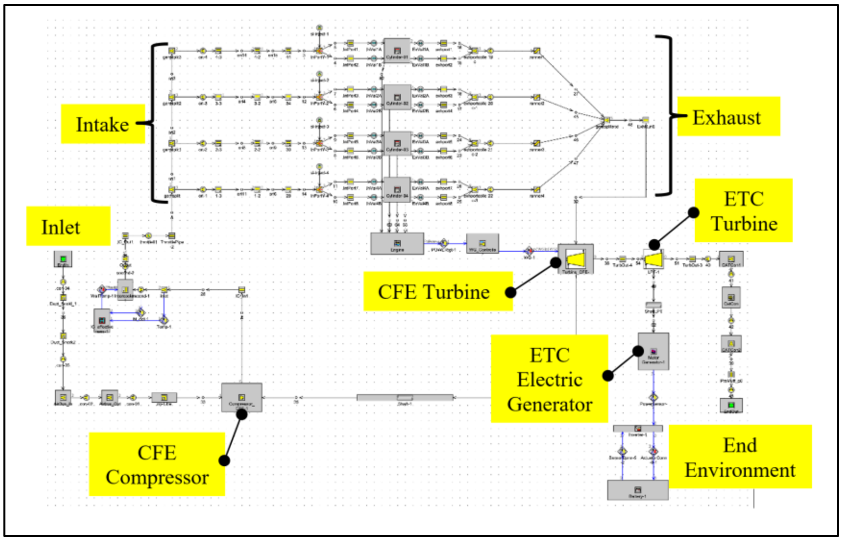

Fig. 2. Model layout of CFE engine with the addition of ETC in GT-Power.

The power generated by the ETC needs to be included in the brake-specific emission calculations for NOx, CO_2, CO, and HC outside of the GT-Power solver, as the exhaust recovery power is not returned to the CFE engine. This value was recalculated using Equation 2. As the engine performance increases as the brake-specific gas emission ($bsGas_i$) decreases.

$$bsGas_i = \left[\frac{m_{gas,i}}{bkw}\right] \times \left[\frac{60000 \times rpm}{n_r}\right] \quad (2)$$

where:

- $m_{gas,i}$ = mass of the gas calculated for (i = NOx, CO_2, CO, and HC)
- bkW = brake engine power
- n_r = revolutions per cycle

RESULTS AND DISCUSSION

Engine Model Validation

Since the combustion model was changed, it was necessary to compare the validated model with the new setup. Fig 3 and Fig 4 show the difference in power and BSFC of the CFE engine before and after changing the combustion model, which shows barely any change. Fig 5 shows the percentage error of the bkW and BSFC between the old and new models more closely. The two models' maximum errors were found to be 0.1% for braking power and 0.01% for BSFC while the average error was 0.01% and 0.005% respectively. With very small errors, the change in the combustion model was acceptable, and the model can be used to add on the ETC for emission analysis in the next stage.

https://doi.org/10.24191/jmeche.v22i2.2928

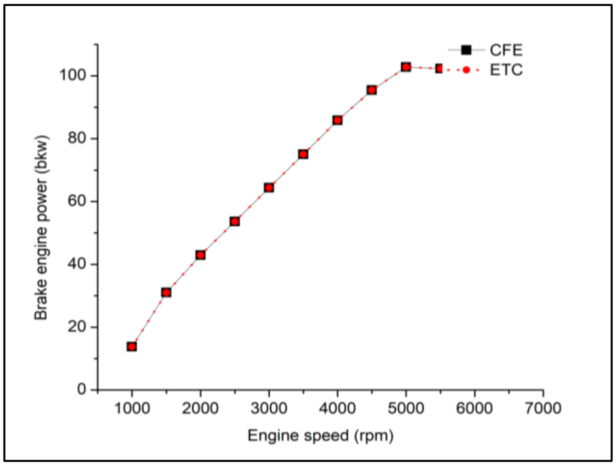

Fig. 3. The difference of brake engine power before and after the combustion model change.

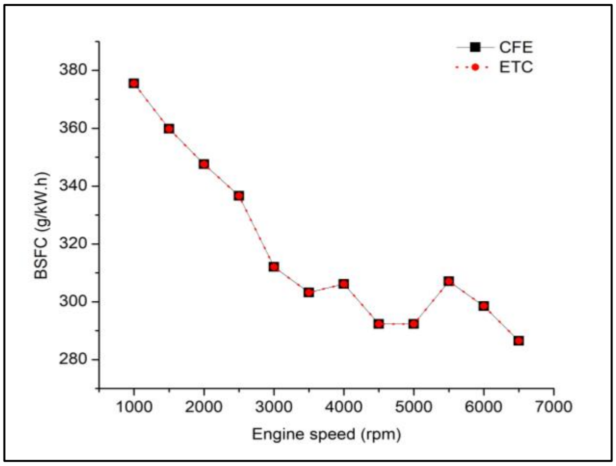

Fig. 4. The difference of Brake Specific Fuel Consumption before and after the combustion model change.

Emissions Analysis

With the included ETC attached to the engine, the simulation was run for the second time to compare the in $bsGas_i$ emissions. The power generated by the ETC is shown in Fig 6. The maximum power of 23.8 kW is generated at 6500 rpm with mostly linear power increase from 1000 rpm to 5000 rpm. As mentioned earlier, a WG was not included in order to limit the energy recovery from the exhaust gas. The objective is to first understand the $bsGas_i$ profile so that the WG can be optimized at a later stage. With the increase in power from the energy recovery, it is expected that most of the emissions should improve.

https://doi.org/10.24191/jmeche.v22i2.2928

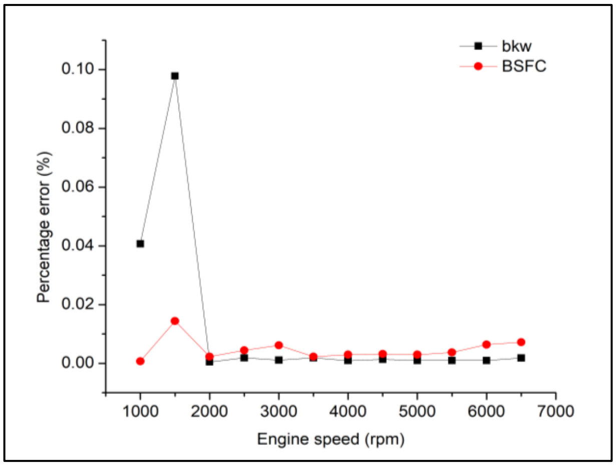

Fig. 5. Percentage error of brake engine power and Brake Specific Fuel Consumption due to combustion model change.

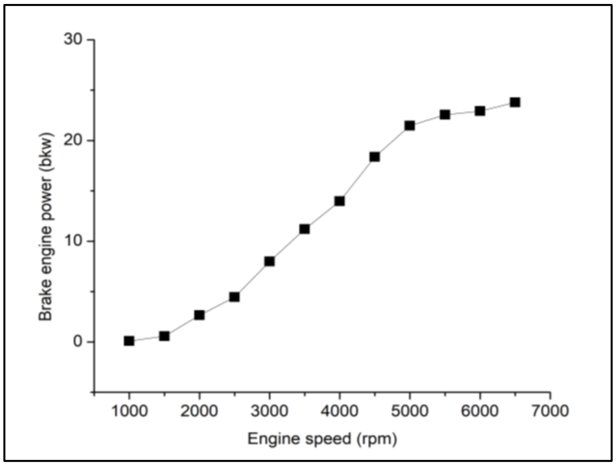

Fig. 6. Power generated by the ETC through exhaust gas energy recovery.

Fig 7 illustrates the difference in brake-specific NOx emissions ($bsGas_{NOx}$)between the engine model equipped with ETC and the original CFE engine. The main improvement can be seen where NOx production is reduced between 2000 rpm and 6500 rpm. This occurs as a result of the exhaust gas's low flow pressure and poor energy recovery at lower rpm, as indicated by the preliminary studies conducted by Muhammad et al. (2018). At higher rpm, there is the greatest reduction in $bsGas_{NOx}$. The largest reduction of 28.8% was seen at 6500 rpm, while the average reduction is 16.17%. The same finding of two-stage turbocharging concludes that the maximum NOx reduction happens at the highest pressure, and another achieves a 25% by using two-stage turbocharging (Sinyavski et al., 2021; Wang et al., 2021).

Fig 8 shows the $bsGas_{CO}$ emission comparison between the two models. The first observation shows that the main improvement is in mid-engine speed between 2000 rpm to 5500 rpm. Even though the energy recovery is higher at the top end, the amount of $bsGas_{CO}$ increases faster after 4500 rpm. Maximum reduction of 7.2% and an average of 4.6%. CO gas is produced due to a lack of oxygen (O_2) in the air

https://doi.org/10.24191/jmeche.v22i2.2928

mixture. At higher speeds, the quantity of air mixture is lacking due to fast combustion timing (Zhai et al., 2020).

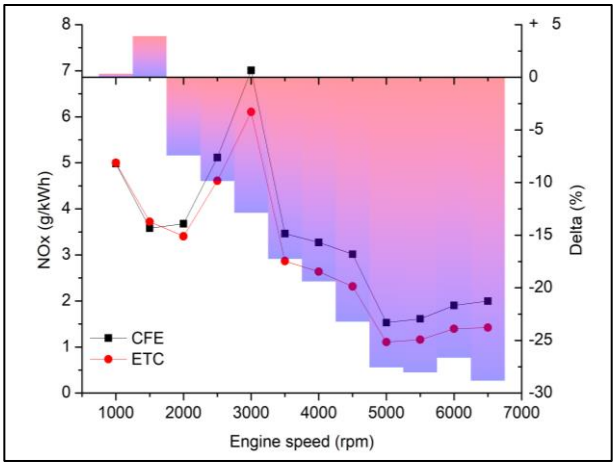

Fig. 7. $bsGas_{NOx}$ emission comparison between the original model and the addition of ETC.

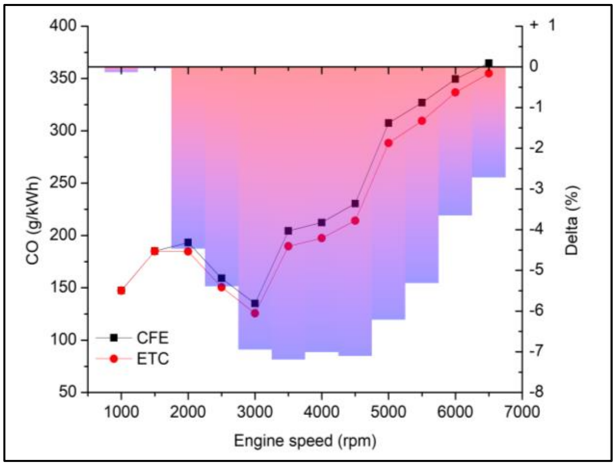

Fig. 8. $bsGas_{CO}$ emission comparison between the original model and the addition of ETC.

By referring to Fig 9, we can see the peak of the reduction is in the window of 3000 rpm to 4500 rpm of $bsGas_{CO2}$. This is in line with another finding of maximum CO_2 reduction at 4500 rpm (Mahmoudi et al., 2017). Average improvement is at 4.3%, with maximum reduction happening at 3500 rpm with 6.9%. Since the engine's optimum torque is in this range, the reduction is likely due to the turbocharger effectively increasing air density, allowing for reduced fuel consumption at this optimal engine speed. In terms of value, CO_2 has more presence compared to other gasses since it's also the byproduct of complete combustion itself (Karczewski et al., 2021).

Some hydrocarbon particles do not react with oxygen due to insufficient oxygen availability and exit the combustion chamber as HC. Fig 10 shows that the $bsGas_{HC}$ is mostly constant between 3000 rpm to 6500 rpm and peaks between 4500 rpm to 5500 rpm. Like the CO, the HC tends to be more prominent at

https://doi.org/10.24191/jmeche.v22i2.2928

high engine speeds, where the combustion is not optimum (Sonthalia et al., 2015). Due to the presence of ETC, the $bsGas_{HC}$ improved a lot in favour of power-to-emission ratio. The average reduction of $bsGas_{HC}$ is 6.9% with a maximum improvement of 9.9% at 4500 rpm.

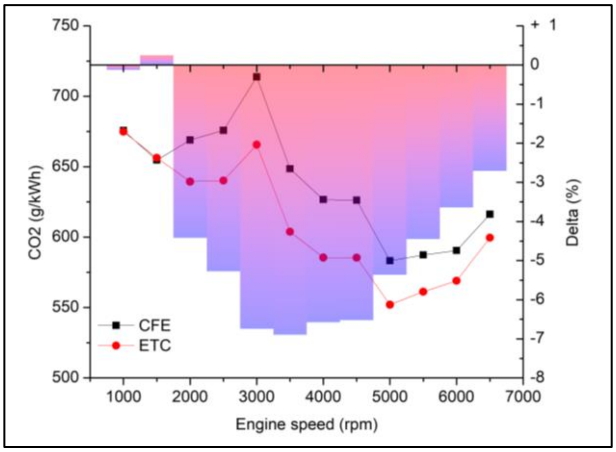

Fig. 9. $bsGas_{CO2}$ emission comparison between the original model and the addition of ETC.

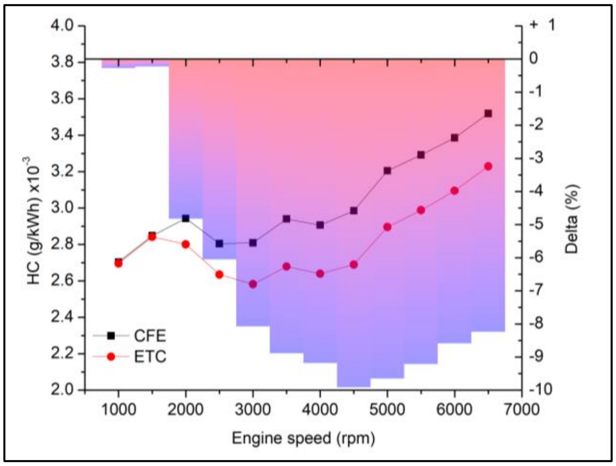

Fig. 10. $bsGas_{HC}$ emission comparison between the original model and the addition of ETC.

CONCLUSION

The overall result shows that all the emissions of the four GHGs have been improved. The maximum reduction achieved was 28.8% in $bsGas_{NOx}$ at 6500 rpm, with more than 4% improvement overall. This improvement was possible due to the energy recovered by the ETC. In summary, the brake-specific emissions decreased overall with the implementation of ETC. By knowing the brake-specific emission profile, further improvement can be made to such a system by improving WG control on the ETC.

https://doi.org/10.24191/jmeche.v22i2.2928

ACKNOWLEDGEMENTS/ FUNDING

The authors would like to acknowledge the support of the College of Engineering, Universiti Teknologi MARA, Shah Alam, Selangor, Malaysia, for providing the facilities and financial support for this research.

CONFLICT OF INTEREST STATEMENT

The authors agree that this research was conducted in the absence of any self-benefits, commercial or financial conflicts and declare the absence of conflicting interests with the funders.

AUTHORS' CONTRIBUTIONS

MHM Muhammad write the manuscript a run the simulation with the help of WSAIW Salim. AMI Mamat devised the project, the main conceptual ideas and the outline. All authors reviewed and approved the final version of this work.

REFERENCE

Alshammari, M., Alshammari, F., & Pesyridis, A. (2019). Electric boosting and energy recovery systems for engine downsizing. Energies, 12(24), 4636.

Benmouna, A., Borderiou, L., & Becherif, M. (2024). Charging stations for large-scale deployment of electric vehicles. Batteries, 10(1), 33.

Carapellucci, R., & Di Battista, D. (2023). Model based evaluation of a turbocharged engine exhaust heat recovery by auxiliary turbine. Proceedings of the ASME 2023 International Mechanical Engineering Congress and Exposition (pp. 1-10). ASME Publisher.

Crippa, M., Guizzardi, D., Pagani, F., Banja, M., Muntean, M., Schaaf, E., Monforti-Ferrario, F., Becker, W., Quadrelli, R., Risquez Martin, A., Taghavi-Moharamli, P., Köykkä, J., Grassi, G., Rossi, S., Melo, J., Oom, D., Branco, A., San-Miguel, J., Manca, G., Pisoni, E., Vignati, E. & Pekar, F., (2024). GHG emissions of all world countries. Publications Office of the European Union.

European Automobile Manufacturers' Association. (2020). CO2 emissions from heavy-duty vehicles. Preliminary CO2 baseline (Q3-Q4 2019) estimate. ACEA Publisher.

Ghojel, J. I. (2010). Review of the development and applications of the Wiebe function: a tribute to the contribution of Ivan Wiebe to engine research. International Journal of Engine Research, 11(4), 297-312.

Ismail, M. I., Costall, A., Martinez-Botas, R., & Rajoo, S. (2015). Turbocharger matching method for reducing residual concentration in a turbocharged gasoline engine. SAE Technical Paper 2015-01-1278, 1-10.

Karczewski, M., Chojnowski, J., & Szamrej, G. (2021). A review of low-CO2 emission fuels for a dual-fuel RCCI engine. Energies, 14(16), 5067.

Lakshminarayanan, P. A. (2024). Two-zone combustion models. In P. A. Lakshminarayanan, A. K.

https://doi.org/10.24191/jmeche.v22i2.2928

Agarwal, H. Ge, & J. M. Mallikarjuna (Eds.), Modelling spark ignition combustion (pp. 13-80). Springer Nature Singapore.

Mahmoudi, A. R., Khazaee, I., & Ghazikhani, M. (2017). Simulating the effects of turbocharging on the emission levels of a gasoline engine. Alexandria Engineering Journal, 56(4), 737-748.

Mamat, A. M. I., Martinez-Botas, R. F., Rajoo, S., Hao, L., & Romagnoli, A. (2016). Design methodology of a low pressure turbine for waste heat recovery via electric turbocompounding. Applied Thermal Engineering, 107, 1166-1182.

Movahed, M. M., Tabrizi, H. B., & Mirsalim, M. (2014). Experimental investigation of the concomitant injection of gasoline and CNG in a turbocharged spark ignition engine. Energy Conversion and Management, 80, 126-136.

Muhammad, M. H. M., Mamat, A. M. I., & Wan Salim, W. S. I. (2018). Exergy analysis of organic Rankine cycle and electric turbo compounding for waste heat recovery. International Journal of Engineering & Technology, 7(3.11), 152-156.

Pakale, P. N., & Patel, S. U. (2015). Performance analysis of IC engine using supercharger and turbocharger - A review. International Journal of Research in Engineering and Technology, 4(2), 17-22.

Serrano, J. R., Climent, H., Piqueras, P., & Darbhamalla, A. (2022). Energy recovery potential by replacing the exhaust gases recirculation valve with an additional turbocharger in a heavy-duty engine. Energy Conversion and Management, 271, 116307.

Silva, C., Ross, M., & Farias, T. (2009). Analysis and simulation of "low-cost" strategies to reduce fuel consumption and emissions in conventional gasoline light-duty vehicles. Energy Conversion and Management, 50(2), 215-222.

Sinyavski, V. V., Krigulski, A. V., Shatrov, M. G., & Golubkov, L. N. (2021). Estimation of nitrogen oxide emission reduction in a boosted truck diesel engine with two-stage charging and Miller cycle. 2021 Intelligent Technologies and Electronic Devices in Vehicle and Road Transport Complex Conference (pp. 1-5). IEEE Publisher.

Sonthalia, A., Rameshkumar, C., Sharma, U., Punganur, A., & Abbas, S. (2015). Combustion and performance characteristics of a small spark ignition engine fuelled with HCNG. Journal of Engineering Science and Technology, 10(4), 404-419.

Wang, P., Hu, Z., Shi, L., Tang, X., Liu, Y., & Deng, K. (2021). Experimental investigation of the effects of Miller timing on performance, energy and exergy characteristics of two-stage turbocharged marine diesel engine. Fuel, 292, 120252.

Zhai, Z., Tu, R., Xu, J., Wang, A., & Hatzopoulou, M. (2020). Capturing the variability in instantaneous vehicle emissions based on field test data. Atmosphere, 11(7), 765.

https://doi.org/10.24191/jmeche.v22i2.2928